Frequent silencing of *RASSF1A* by DNA methylation in thymic neuroendocrine tumours

Koichiro Kajiura[1,3], kkajiura7@ybb.ne.jp

Hiromitsu Takizawa[1], h-takizawa@mbf.ocn.ne.jp

Yuki Morimoto[2], morimoto.yuuki@tokushima-u.ac.jp

Kiyoshi Masuda[3], kiyoshim@tokushima-u.ac.jp

Mitsuhiro Tsuboi[1], tsuboi.mitsuhiro@tokushima-u.ac.jp

Reina Kishibuchi[2] , x6911xlthl@gmail.com

Nuliamina Wusiman[2], uyghur.amina@gmail.com

Toru Sawada[1], sawada.tooru@tokushima-u.ac.jp

Naoya Kawakita[1], kawakita.naoya@tokushima-u.ac.jp

Hiroaki Toba[1], ht1109@tokushima-u.ac.jp

Mitsuteru Yoshida[1], mitsuteru@tokushima-u.ac.jp

Yukikiyo Kawakami[1], y-kawakami@tokushima-u.ac.jp

Takuya Naruto[3], naruto.takuya@tokushima-u.ac.jp

Issei Imoto[3], issehgen@tokushima-u.ac.jp

Akira Tangoku[1], tangoku@tokushima-u.ac.jp

Kazuya Kondo[2] , kzykondo@tokusima-u.ac.jp

[1]Department of Thoracic, Endocrine and Oncological Surgery, Graduate School of Biomedical Sciences, Tokushima University Graduate School, Tokushima city 770-8503, Japan.

[2]Department of Oncological Medical Services, Graduate School of Biomedical Sciences, Tokushima University Graduate School, Tokushima city 770-8503, Japan.

[3]Department of Human Genetics, Graduate School of Biomedical Sciences, Tokushima University Graduate School, Tokushima city 770-8503, Japan.

Correspondence: Hiromitsu Takizawa

e-mail: h-takizawa@mbf.ocn.ne.jp

Abstract

Objectives: Aberrant methylation of promoter CpG islands (CGIs) of tumour suppressor genes is a common epigenetic mechanism underlying cancer pathogenesis. The methylation patterns of thymic tumours have not been studied in detail since such tumours are rare. Herein, we sought to identify genes that could serve as epigenetic targets for thymic neuroendocrine tumour (NET) therapy.

Materials and Methods: Genome-wide screening for aberrantly methylated CGIs was performed in three NET samples, seven thymic carcinoma (TC) samples, and eight type-B3 thymoma samples. The methylation status of thymic epithelial tumours (TETs) samples was validated by pyrosequencing in a larger cohort. The expression status was analysed by quantitative polymerase chain reaction (PCR) and immunohistochemistry.

Results: We identified a CGI on a novel gene, *RASSF1A,* which was strongly hypermethylated in NET, but not in thymic carcinoma or B3 thymoma. *RASSF1A* was identified as a candidate gene statistically and bibliographically, as it showed frequent CGI hypermethylation in NET by genome-wide screening. Pyrosequencing confirmed significant hypermethylation of a *RASSF1A* CGI in NET. Low-grade NET tissue was more strongly methylated than high-grade NET. Quantitative PCR and immunohistochemical staining revealed that RASSF1A mRNA and protein expression levels were negatively regulated by DNA methylation.

Conclusions: *RASSF1A* is a tumour suppressor gene epigenetically dysregulated in NET. Aberrant methylation of *RASSF1A* has been reported in various tumours, but this is the first report of *RASSF1A* hypermethylation in TETs. *RASSF1A* may represent an epigenetic therapeutic target in thymic NET.

Keywords: *RASSF1A*, thymic neuroendocrine tumor, DNA methylation

1. Introduction

The 4th edition of the World Health Organization (WHO) Classification of tumours of the lung, pleura, thymus, and heart classified typical and atypical carcinoids as low-grade and intermediate-grade thymic neuroendocrine tumours (NETs), respectively, and distinguished them from high-grade neuroendocrine carcinomas (NECs), which, in turn, comprised large-cell neuroendocrine carcinomas and small-cell carcinomas [1]. The overall survival rates of NET and thymic carcinoma (TC) patients are lower than that of thymoma patients [2,3]. However, the biological features of thymic epithelial tumours (TETs), including NETs, have not been elucidated because these are rare tumours, preventing the development of effective therapeutic strategy, though the TET staging system had been established based on the survival and recurrence rates by the International Association for the Study of Lung Cancer and the International Thymic Malignancies Interest Group [4,5,6,7]. It is therefore necessary to identify biomarkers that could be used for the early detection of these cancers and for the development of novel targeted therapies to improve the survival rate.

Aberrant methylation of promoter CpG islands (CGIs) of tumour suppressor genes has been established as a common epigenetic mechanism underlying the pathogenesis of various cancers in humans, including lung adenocarcinoma [8,9,10]. However, there have been no reports about the DNA methylation pattern in thymic epithelial tumours (TETs) because this type of cancer, especially NET, is relatively rare. In the present study, we performed a systematic, genome-wide screening of aberrantly methylated CGIs in NET, TC, and B3 thymoma samples to identify commonly dysregulated genes. In addition, we aimed to identify novel genes that could serve as epigenetic targets for NET therapy.

2. Methods

2.1. Primary tissue sample collection

In total, 51 thymic tumour samples and 10 paired normal tissues were obtained from patients with histologically proven TET, who underwent surgery at the Tokushima University

Hospital (Tokushima, Japan) between 1990 and 2016. The breakdown of 51 thymic tumour samples by diagnosis was as follows: NET, 11 samples; TC, 11 samples; type B3 thymoma, 9 samples; type B2 thymoma, 7 samples; type B1 thymoma, 5 samples; type AB thymoma, 5 samples; and type A thymoma, 3 samples. DNA methylation genome-wide screening was carried out with a HumanMethylation450K array. Pyrosequencing-based methylation analysis validated the methylation status of the candidate gene. Expression was analysed by quantitative PCR and immunohistochemistry (Table 1, Supplementary Table 1).

Tumours were snap-frozen and stored at −80 °C until required for DNA and RNA analysis. Tumour specimens were characterised according to Masaoka-Koga [11] and WHO classifications [12]. Diagnosis was verified by histopathology.

This study was performed in accordance with the principles outlined in the Declaration of Helsinki. Following the approval of all aspects of these studies by the local ethics committee (Tokushima University Hospital, approval numbers 2205-1, 2228), formal written consent was obtained from all patients.

2.2. DNA and RNA preparation and bisulphite conversion of genomic DNA

DNA and RNA were extracted using standard methods. Bisulphite conversion of DNA was conducted using an EZ DNA Methylation Gold kit (Zymo Research, Irvine, CA, USA).

2.3. Global methylation analysis

HumanMethylation450K BeadChip (Illumina, Santa Clara, CA, USA) analysis was performed according to the manufacturer's instructions. The default settings of the GenomeStudio software DNA methylation module (Illumina) were applied to calculate the methylation levels of CpG sites as β-values ($\beta = \text{intensity}_{\text{methylated}}/\text{intensity}_{\text{methylated + unmethylated}}$). The data were further normalised using the peak correction algorithm embedded in the Illumina Methylation Analyzer (IMA) R package [8]. To identify CGIs differentially methylated in NET and TC samples in the discovery set, median-averaged β-differences in

CGI-based regions were calculated based on a matrix of β-differences, in which β-values of TC samples were subtracted from those of NET samples. The statistical significance of these differences was evaluated using Welch's *t*-test in IMA. Multiple testing corrections were performed using the Benjamini–Hochberg approach, with significantly differential methylation defined as a false discovery rate (FDR)-adjusted *P*-value < 0.05. The following criteria were used for differentially methylated CGIs: β-difference > 0.5 and FDR-adjusted *P*-value < 0.05. Methylation data for the discovery cohort were deposited in the Gene Ontology Database under accession number GSE94769.

2.4. Bisulphite pyrosequencing

Bisulphite-treated genomic DNA was amplified using a set of primers designed with the PyroMark Assay Design software (version 2.0.01.15; Qiagen, Valencia, CA, USA; Supplementary Table 4). PCR product pyrosequencing and methylation quantification were performed with a PyroMark 24 Pyrosequencing System, version 2.0.6 (Qiagen) with sequencing primers designed according to the manufacturer's instructions.

2.5. Quantitative PCR

Quantitative PCR (qPCR) was performed using a TaqMan gene expression assay kit (Supplementary Table 4) according to the manufacturer's instructions. *GAPDH* mRNA levels were used as the internal controls for normalization.

2.6. Immunohistochemical staining

Paraffin-embedded sections (thickness, 4 μm) were heated in a microwave oven for 20 min for antigen retrieval. A CSA II kit (DAKO Japan, Tokyo, Japan) and a primary antibody against RASSF1A (Supplementary Table 4) were used according to the manufacturer's instructions [9]. The intensity and expansion of *RASSF1A* stain in the NET, TC, and B3 samples were scored. We defined stain score as the sum of the intensity and expansion

scores. A stain score of ≤2 indicated inhibition of protein expression. Immunohistochemical (IHC) data scoring was performed independently by two different researchers.

2.7. Statistical analysis

Results are expressed as the mean ± standard deviation. Welch's *t*-test or unpaired Student's *t*-test was used for comparisons between two groups. Mann–Whitney *U* test was used for comparisons between non-paired samples, when data were not normally distributed. The relation between continuous variables was investigated by calculating the Pearson's correlation coefficient. Differences were assessed by using two-sided tests and were considered significant at a *P*-value of <0.05. Statistical analyses were performed using R 3.2.2 (R Project for Statistical Computing, Vienna, Austria).

3. Results

3.1. Screening of aberrantly methylated CGIs in tumour samples

We initially screened three NET samples, seven TC samples, and eight B3 thymoma samples obtained from freshly frozen specimens (Table 1, Supplementary Table 1) with an Illumina HumanMethylation450K BeadChip to identify differentially methylated CGIs in a genome-wide manner. A volcano plot showed that, in NET samples, the number of significantly different and hypermethylated CGIs was much larger than the number of hypomethylated CGIs, which was in contrast to the results obtained for TC or B3 thymoma samples (Fig. 1A, B). Thirty-five CGIs were identified as differentially hypermethylated in the NET samples in relation to the TC samples (FDR < 0.05 and β difference [NET – TC] > 0.5). Furthermore, 39 CGIs were identified as differentially hypermethylated in the NET samples compared with the B3 thymoma samples using the same statistical criteria. *RASSF1A* was among the top 15 differentially methylated genes in the NET samples compared with the TC (Supplementary Table 2) and B3 thymoma (Supplementary Table 3) samples. In addition, we identified ten genes as commonly hypermethylated in NET (Fig. 1C). *RASSF1A* was one

of the most significant hypermethylated genes in the NET samples.

3.2. CGI methylation status of the RASSF1A promoter in TETs

Using the methylation array data of 22 TET samples (three NET samples, seven TC samples, eight B3 thymoma samples, three thymoma A samples, and one normal thymus tissue sample), we analysed the methylation status of CpG sites within *RASSF1A* [10]. CpG sites within the CGI exhibited low levels of methylation in samples from TC, thymomas, and normal thymic tissue. In contrast, significantly higher methylation levels were detected in the NET samples in all CpG sites (Fig. 2A).

Quantitative pyrosequencing analysis of five target CpG sites within the *RASSF1A* CGI revealed very low methylation levels in all five CpG sites in the TC, thymoma, and normal thymic tissue samples, whereas the NET samples exhibited high levels of DNA methylation (Fig. 2B). Therefore, the DNA methylation levels in the NET samples in all five *RASSF1A* CpG sites were significantly different from those in samples from other TETs or from normal thymic tissue.

Pyrosequencing demonstrated that low-grade and intermediate-grade NETs, known as typical and atypical carcinoids, respectively, had significantly ($P = 1.53 \times 10^{-9}$) hypermethylated CpG sites on *RASSF1A* promoter region cg21554552 (II) compared to their methylation level in NECs (Fig. 3A).

3.3. Expression of RASSF1A in TETs

QPCR analysis showed that the *RASSF1A* mRNA expression level was lower in NETs than in other TETs and normal thymic tissue (Fig. 4A). There was a negative correlation between the extent of methylation of CpG sites and *RASSF1A* expression levels in cg21554552 (II) in TETs and normal thymic tissue (Fig. 4B). Apparently, DNA methylation of the *RASSF1A* promoter region regulated *RASSF1A* mRNA expression. To evaluate the RASSF1A protein expression level in TET, IHC staining was performed (Fig. 5A).

Cytoplasmic RASSF1A staining was observed in tumour cells of TC and B3 thymoma, whereas almost no RASSF1A staining was observed in NET cells. IHC analysis of scores of staining intensity and expansion of RASSF1A-specific stain showed that RASSF1A protein expression was significantly (P = 0.02) inhibited in NETs.

4. Discussion

In this present study, we performed genome-wide screening of various thymic tumours, including NETs, to identify novel genes that could be epigenetic therapeutic targets. We focused on the methylation status and expression level of *RASSF1A,* one of the ten candidate genes that exhibited significantly higher methylation levels in NET samples than in TC or B3 thymoma specimens. The methylation analysis revealed that the promoter region of *RASSF1A* was significantly methylated in NETs compared to in TC and/or B3 thymoma. The expression levels of RASSF1A mRNA and protein were inhibited in NETs compared to in other TETs and/or normal thymus tissues. DNA methylation of the *RASSF1A* promoter region regulated the expression of *RASSF1A* in thymic NETs.

RASSF1 is a member of the *RASSF* family (*RASSF1–8*). This gene gives rise to eight different isoforms due to alternative splicing and alternative promoter usage [14]. In contrast to RAF and phosphatidylinositol 3-kinase, which are *RAS* effectors that specifically bind the GTP-bound form of *RAS* and control proliferation and survival, RASSF proteins are known as tumour suppressors because they induce cell cycle arrest, mitotic arrest, and apoptosis [14,15,16]. Loss of *RASSF1A* expression is largely attributed to promoter hypermethylation, as somatic mutations of *RASSF1A* are uncommon, although several polymorphisms have been detected [17]. Frequently, high level of DNA methylation of the promoter region and low expression of *RASSF1A* have been associated with negative prognosis of neuroendocrine tumours of other organs such as the pancreas, gastrointestinal tract, bronchi, or lungs [15,16,18,19,20]. However, to the best of our knowledge, the present study is the first to report the inverse relationship between the DNA methylation status of

RASSF1A and its expression level in thymic tumours, including NETs. Our results suggest that *RASSF1A* might be a novel epigenetic target of cancer therapy.

Besides *RASSF1A*, our study identified several other genes that could be candidate molecular targets for the epigenetic modification therapy of thymic NET (Fig. 1C). The protein product of *SKI* represses TGF-β-induced epithelial-mesenchymal transition and invasion by inhibiting SMAD-dependent signalling in non-small cell lung cancer [21]. The transmembrane 106A gene (*TMEM106A*) is a novel tumour suppressor gene silenced by DNA methylation in gastric cancer [22]. Palladin, encoded by *PALLD*, regulates the ability of cancer cells to become invasive and metastatic [23]. The latent transforming growth factor β-binding protein gene (*LTBP4*) is downregulated in adenocarcinomas and squamous cell carcinomas in oesophageal cancer [24]. Gene fusions of *THAP4* with *VAV1* (*VAV1-THAP4*) generate recurrent in-frame deletions (VAV1 Δ778-786) by a focal deletion-driven alternative splicing mechanism in peripheral T-cell lymphomas [25]. GNG8 is involved in the WNT/β-catenin- and G protein-coupled receptor signalling pathways in chronic lymphocytic leukaemia and small lymphocytic lymphoma [26]. *TMEM37* is likely to be methylated as a consequence of rat mammary carcinogenesis, but it is not expressed in normal mammary glands [27]. *SRRM3* may be involved in breast cancer progression mediated by RING1 and YY1-binding protein [28]. Therefore, *SKI, TMEM106A, PALLD, LTBP4, THAP4, GNG8,* and *SRRM3* may be candidate genes for epigenetic target therapy, in addition to *RASSF1A*.

Nowadays, it is possible to demethylate targeted CpG sites in regulatory regions using fusion proteins containing the dCas9-peptide repeat and the scFv-TET1 catalytic domain [29]. This new technology has applications in the development of epigenetic target therapy for various cancers. Therefore, it is necessary to identify target CpG sites and/or epigenetically controlled regions on driver genes. The results of this study might aid the development of targeted therapy for thymic NETs.

There are several limitations to this study. First, type B1 and B2 thymomas were excluded from our methylation and expression analysis, because these tumours were

infiltrated by large quantities of lymphocytes, and we could not selectively analyse epithelial tumour cells. Second, apart from *RASSF1A*, we could not survey the other candidate genes in detail. We focused on *RASSF1A* in this study as this gene has been reported to be hypermethylated in NETs of other organs such as pancreas, gastrointestinal tract, bronchi, and lungs [15,16,18,19,20]. Third, only a small cohort of NET samples was used for the genome-wide analysis. This small sample size might not have been sufficient to detect all epigenetically controlled candidate genes. In addition, it was unclear whether the expression of *RASSF1A* could play role in the prognosis in thymic NETs. Finally, we did not perform functional assays for RASSF1A in the thymus.

In conclusion, the expression of *RASSF1A*, a known tumour-suppressor gene, was found to be epigenetically controlled in thymic NETs as well as NETs of other tissues. Our results suggest that *RASSF1A* is a candidate gene for epigenetic target therapy.

Disclosure of Potential Conflicts of Interest

The authors have no conflicts of interest to declare.

Acknowledgments

Several NET samples were kindly provided by Koichiro Kenzaki and Tetsuro Ogino of the Takamatsu Red Cross Hospital, Japan. A sample of NET was provided by Hisashi Matsuoka of the Kochi Red Cross Hospital.

Funding: This work was supported in part by the Japan Society for the Promotion of Science KAKENHI [grant numbers 25861245 (K.K.), 26462145 (Y.N.)].

References

1. A. Marx, JKC. Chan, JM. Coindre, F. Detterbeck, N. Girard, NL. Harris, et al., The 2015 world health organization classification of tumor of the thymus, J Thorac Oncol 10 (2015) 1383-1395. DOI: 10.1097/JTO.000000000000065
2. PL. Filosso, X. Yao, E. Ruffini, U. Ahmad, A. Antonicelli, J. Huang, et al., Comparison of outcomes between neuroendocrine thymic tumours and other subtypes of thymic carcinomas: a joint analysis of the European society of thoracic surgeons and the international thymic malignancy interest group, Eur J Cardiothorac Surg 50 (2016) 766-71. doi:10.1093/ejcts/ezw107
3. K. Kondo, Y. Monden, Therapy for thymic epithelial tumors: A clinical study of 1,320 patients from Japan, Ann Thorac Surg 76 (2003) 878-85.
4. FC. Detterbeck, K. Stratton, D. Giroux, H. Asamura, J. Crowley, C. Falkson, et al., The IASLC/ITMIG thymic epithelial tumors staging project : proposal for an evidence-based stage classification system for the forthcoming (8th) edition of the TNM classification of malignant tumors, J Thorac Oncol 9 (2014) S65-S72.
5. AG. Nicholson, FC. Detterbeck, M. Marino, J. Kim, K. Stratton, D. Giroux, et al., The IASLC/ITMIG thymic epithelial tumors staging project : proposals for the T component for the forthcoming (8th) edition of the TNM classification of malignant tumors, J Thorac Oncol 9 (2014) S73-S80.
6. K. Kondo, PV. Schil, FC. Detterbeck, M. Okumura, K. Stratton, D. Giroux, et al., The IASLC/ITMIG thymic epithelial tumors staging project : proposals for the N and M components for the forthcoming (8th) edition of the TNM classification of malignant tumors, J Thorac Oncol 9 (2014) S81-S87.
7. FY. Bhora, DJ. Chen, FC. Detterbeck, H. Asamura, C. Falkson, PL. Filosso, et al., The IASLC/ITMIG thymic epithelial tumors staging project : a proposed lymph node map for thymic epithelial tumors in the forthcoming 8th edition of the TNM classification of malignant tumors, J Thorac Oncol 9 (2014) S88-S96.

8. K. Kajiura, K. Masuda, T. Naruto, T. Kohmoto, M. Watanabe, M. Tsuboi, et al., Frequent silencing of the candidate tumor suppressor TRIM58 by promoter methylation in early-stage lung adenocarcinoma, Oncotarget 8 (2016) 2890-2905. **DOI: 10.18632/oncotarget.13761**
9. H. Izumi, J. Inoue, S. Yokoi, H. Hosoda, T. Shibata, M. Sunamori, et al., Frequent silencing of DBC1 is by genetic or epigenetic mechanisms in non-small cell lung cancers, Hum Mol Genet 14 (2005) 997–1007. doi:10.1093/hmg/ddi092
10. I. Imoto I, H. Izumi, S. Yokoi, H. Hosoda, T. Shibata, F. Hosoda, et al., Frequent silencing of the candidate tumor suppressor PCDH20 by epigenetic mechanism in non-small-cell lung cancers, Cancer Res. 66 (2006) 4617–4626. doi:10.1158/0008-5472.CAN-05-4437
11. FC. Detterbeck, AG. Nicholson, K. Kondo, PV. Schil, C. Moran, The Masaoka-Koga stage classification for thymic malignancy, J Thorac Oncol 6 (2011) S1710–S1716.
12. A. Marx, P. Strobel, SB. Badve, L. Chalabreysse, JKC. Chan, G. Chen, et al., ITMIG consensus statement on the use of the WHO histological classification of thymoma and thymic carcinoma: refined definitions, histological criteria, and reporting, J Thorac Oncol 9 (2014) 596–611.
13. A. Honjo, H. Ogawa, M. Azuma, T. Tezuka, S. Sone, A. Biragyn, et al., Targeted reduction of CCR4+ cells is sufficient to suppress allergic airway inflammation, Respir Investig 51 (2013) 241-249. doi: 10.1016/j.resinv.2013.04.007.
14. H. Donninger, MD. Vos, GJ. Clark, The RASSF1A tumor suppressor, J Cell Sci 120 (2007) 3163-3172. doi:10.1242/jcs.010389
15. A. Karpathakis, H. Dibra, C. Thirlwell, Neuroendocrine tumours: cracking the epigenetic code, Endocr Relat Cancer 20 (2013) R65-R82. DOI: 10.1530/ERC-12-0338
16. P. Mapelli, EO. Aboagye, J. Stebbing, R. Sharma, Epigenetic changes in gastroenteropancreatic neuroendocrine tumours, *Oncogene* (2014) 1-9. doi: 10.1038/onc.2014.379
17. L.van der Weyen, D.J. Adams, The Ras-association domain family (RASSF) members

and their role in human tumourigenesis, Biochim Biophys Acta. 1776 (2007) 58–85.

18. HY. Zhang, KM. Rumilla, L. Jin, N. Nakamura, GA. Stilling, KH. Ruebel, et al., Association of DNA methylation and epigenetic inactivation of *RASSF1a* and Beta-catenin with metastasis in small bowel carcinoid tumors, Endocrine 30 (2006) 299-306.
19. G. Pelosi, C. Fumagalli, M. Trubia, A. Sonzogni, N. Rekhtman, P. Maisonneuve, et al., Dual role of RASSF1 as a tumor suppressor and an oncogene in neuroendocrine tumors of the lung, Anticancer RES 30 (2010) 4269-4282.
20. L. Liu, RR. Broaddus, JC. Yao, S. Xie, JA. White, TT. Wu, et al., Epigenetic alternations in neuroendocrine tumors: methylation of RAS-association domain family 1, isoform A and p16 genes are associated with metastasis, Mod Pathol 18 (2005) 1632–1640. doi:10.1038/modpathol.3800490
21. H. Yang, L. Zhan, T. Yang, L. Wang, C. LI, J. ZHAO, et al., Ski prevents TGF-β-induced EMT and cell invasion by repressing SMAD-dependent signaling in non-small cell cancer, Oncol Rep 34 (2015) 87-94. DOI: 10.3892/or.2015.3961
22. D. Xu, L. Qu, J. Hu, G. Li, P. Lv, D. Ma, et al., Transmembrane protein 106A is silenced by promotor region hypermethylation and suppresses gastric cancer growth by inducing apoptosis, J Cell Mol Med 18 (2014) 1655-1666. doi: 10.1111/jcmm.12352
23. R. Yadav, R. Vattepu, MR. Beck, Phosphoinositides binding inhibits actin crosslinking and polymerization by Palladin, J Mol Biol 428 (2016) 4031–4047. Doi.org/10.1016/j.jmb.2016.07.018
24. I. Bultmann, A. Conradi, C. Kretschmer, A. Sterner-Kock, Latent transforming growth factor β-binding protein 4 is downregulated in esophageal cancer via promotor methylation, PLoS ONE 8 (2013) e65614. doi:10.1371/journal.pone.0065614
25. F. Abate, AC. Silva-Almeida, S. Zairis, J. Robles-Valero, L. Couronne, H. Khiabanian, et al., Activating mutations and translocations in the guanine exchange factor VAV1 in peripheral T-cell lymphomas, PNAS (2017).

www.pnas.org/cgi/doi/10.1073/pnas.1608839114

26. FCM. Sille, R. Thomas, MT. Smith, L. Conde, CF. Skibola, Post-GWAS functional characterization of susceptibility variants for chronic lymphocytic leukemia, PLoS ONE 7 (2012) e29632. doi:10.1371/journal.pone.0029632
27. N. Hattori, E. Okochi-Takada, M. Kikuyama, M. Wakabayashi, S. Yamashita, T. Ushijima, Methylation silencing of angiopoietin-like 4 in rat and human mammary carcinomas, Cancer Sci 102 (2011) 1337-1343.
28. H. Zhou, J. Li, Z. Zhang, R. Ye, N. Shao, T. Cheang, et al., RING1 and YY1 binding protein suppresses breast cancer growth and metastasis, Int J Oncol 49 (2016) 2442-2452. Doi:10.3892/ijo.2016.3718
29. S. Morita, H. Noguchi, T. Horii, K. Nakabayashi, M. Kimura, K. Okamura, et al., Targeted DNA demethylation in vivo using dCas9-peptide repeat and scFv-TET1 catalytic domain fusions., Nat Biotechnol 34 (2016) 1060-1065. doi: 10.1038/nbt.3658

Figure captions

Fig. 1. *RASSF1A* is a candidate gene with selective hypermethylation of CpG islands (CGIs) in thymic neuroendocrine tumours (NETs).

A. Volcano plot of the differential CGI methylation profiles of three NET and seven thymic carcinoma samples. The x-axis indicates the average β-value difference (methylation level). The y-axis indicates the $-\log_{10}$ value of the adjusted Welch's test *P*-value for each CGI. The arrow indicates the CGI around *RASSF1A*.

B. Volcano plot of the differential CGI methylation profiles of three NET and eight B3s thymoma samples. The x-axis indicates the average β-value difference (methylation level). The y-axis indicates the $-\log_{10}$ value of the adjusted Welch's test *P*-value for each CGI. The arrow indicates the CGI around *RASSF1A*.

C. The top 15 genes, whose methylation status was significantly different in NET vs. TC samples and in NET vs. B3 thymoma samples according to the following criteria: false discovery rate (FDR) < 0.05; β difference (NET – TC) > 0.5. The methylation status of ten genes was significantly different in NET samples in comparison with TC and B3 thymoma samples.

Fig. 2. Methylation status of *RASSF1A* in thymic epithelial tumours (TETs).

A. A schematic diagram of the *RASSF1A* structure and CpG sites around exon 1α. Average β-values indicating the methylation level of each CpG site are indicated. The array-based methylation experiment involved three NET samples, seven TC samples, eight B3 thymoma samples, three thymoma A samples, and one normal thymic tissue sample. The CpG sites around exon 1α on the promoter region targeted by pyrosequencing are shown as I–V.

B. Average DNA methylation rates of five target sites indicated in **A** obtained by quantitative pyrosequencing of TETs, including NETs.

Fig. 3. DNA methylation levels in thymic tumours of different grades.

DNA methylation levels of cg21554552 (target II in Fig. 2A, B) were analysed by quantitative pyrosequencing in low-grade and intermediate-grade NETs as well as in high-grade neuroendocrine carcinomas. The dotted line indicates a methylation level of 0.3. Samples were defined as being hypermethylated at cg21554552 if the methylation rate was above 0.3.

Fig. 4. *RASSF1A* mRNA expression level in TET.

A. Boxplot of the relative *RASSF1A* mRNA expression levels (fold change) in TET samples, as determined by quantitative polymerase chain reaction (qPCR). Data were normalised to *GAPDH* mRNA levels and are expressed as the mean ± standard deviation of experiments performed in triplicate.

B. Correlation between the methylation rate of the CpG site cg21554552 (II) and *RASSF1A* expression level. The x-axis indicates the methylation level determined by pyrosequencing. The y-axis indicates the *RASSF1A* mRNA expression level determined by qPCR and normalised to that of *GAPDH*.

Figure 5. RASSF1A protein expression level in TET.

A. Representative images of immunohistochemical staining for RASSF1A in NET, TC, and B3 thymoma samples. Scale bars, 200 μm.

B. Scores of the intensity and expansion of RASSF1A-specific stain in NET, TC, and B3 thymoma samples. Staining score = intensity score + expansion score. Protein expression was considered to be inhibited if the stain score was ≤2.

Figure 1

A

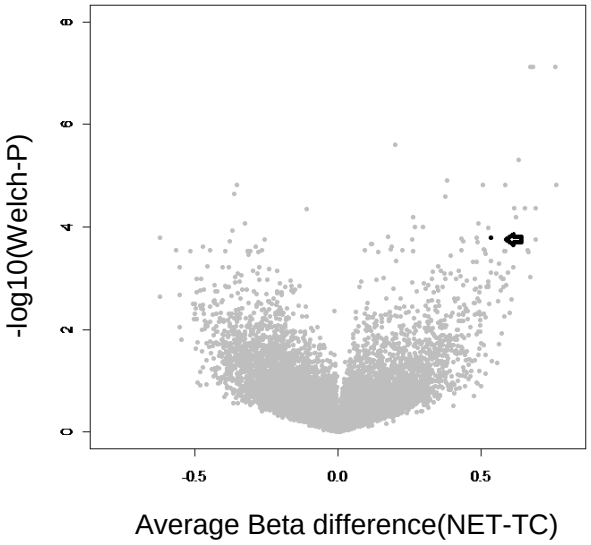
-log10(Welch-P)
0
2
4
6
8
-0.5
0.0
0.5
Average Beta difference(NET-TC)

B

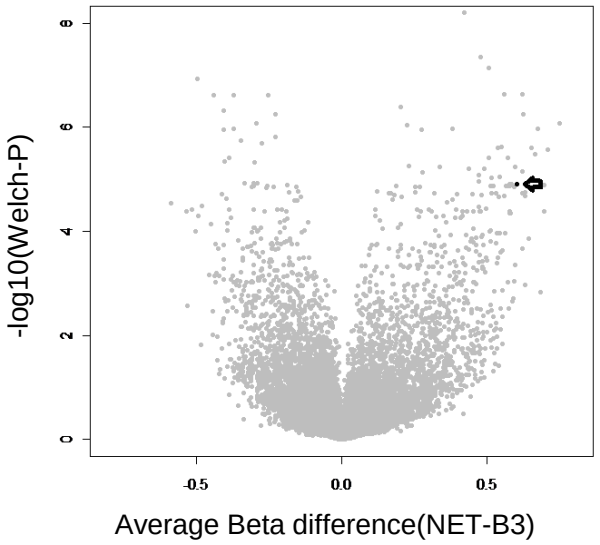
-log10(Welch-P)
0
2
4
6
8
-0.5
0.0
0.5
Average Beta difference(NET-B3)

C

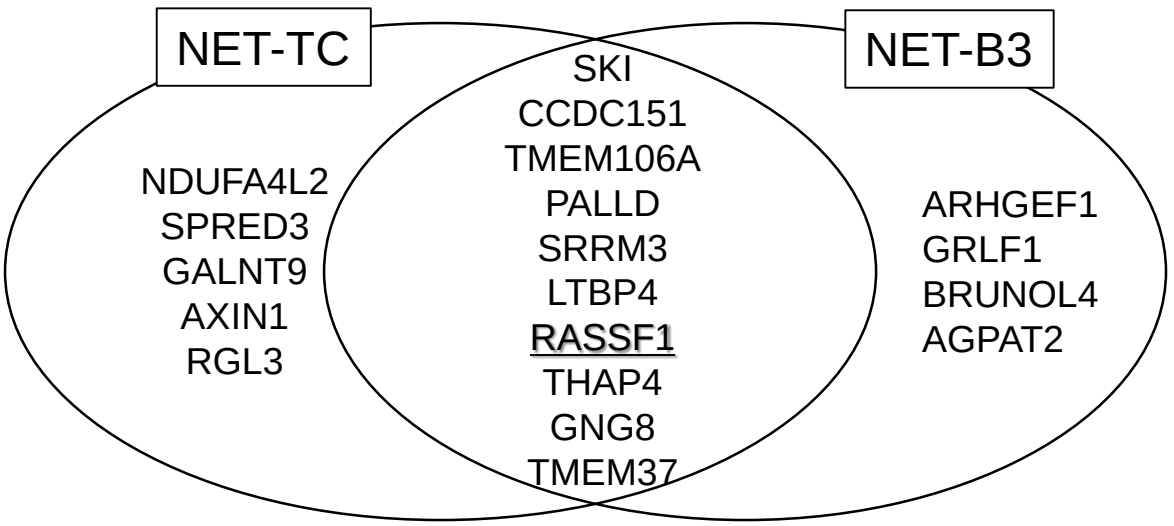
NET-TC
NET-B3
NDUFA4L2
SPRED3
GALNT9
AXIN1
RGL3
SKI
CCDC151
TMEM106A
PALLD
SRRM3
LTBP4
RASSF1
THAP4
GNG8
TMEM37
ARHGEF1
GRLF1
BRUNOL4
AGPAT2

Figure 2

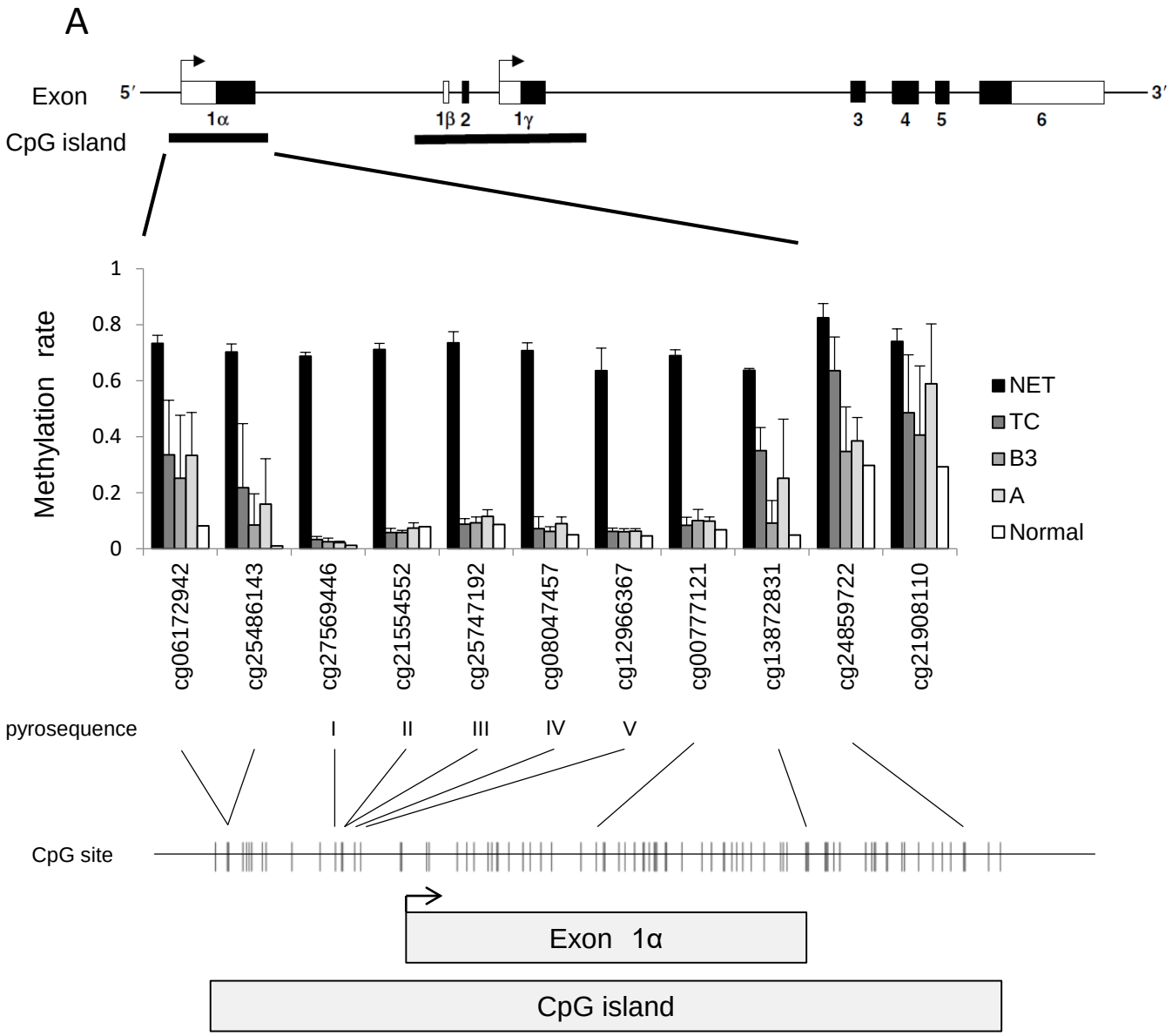
A
Exon
5′
3′
1α
1β 2
1γ
3
4
5
6
CpG island
Methylation rate
1
0.8
0.6
0.4
0.2
0
NET
TC
B3
A
Normal
cg06172942
cg25486143
cg27569446
cg21554552
cg25747192
cg08047457
cg12966367
cg00777121
cg13872831
cg24859722
cg21908110
pyrosequence
I
II
III
IV
V
CpG site
Exon 1α
CpG island

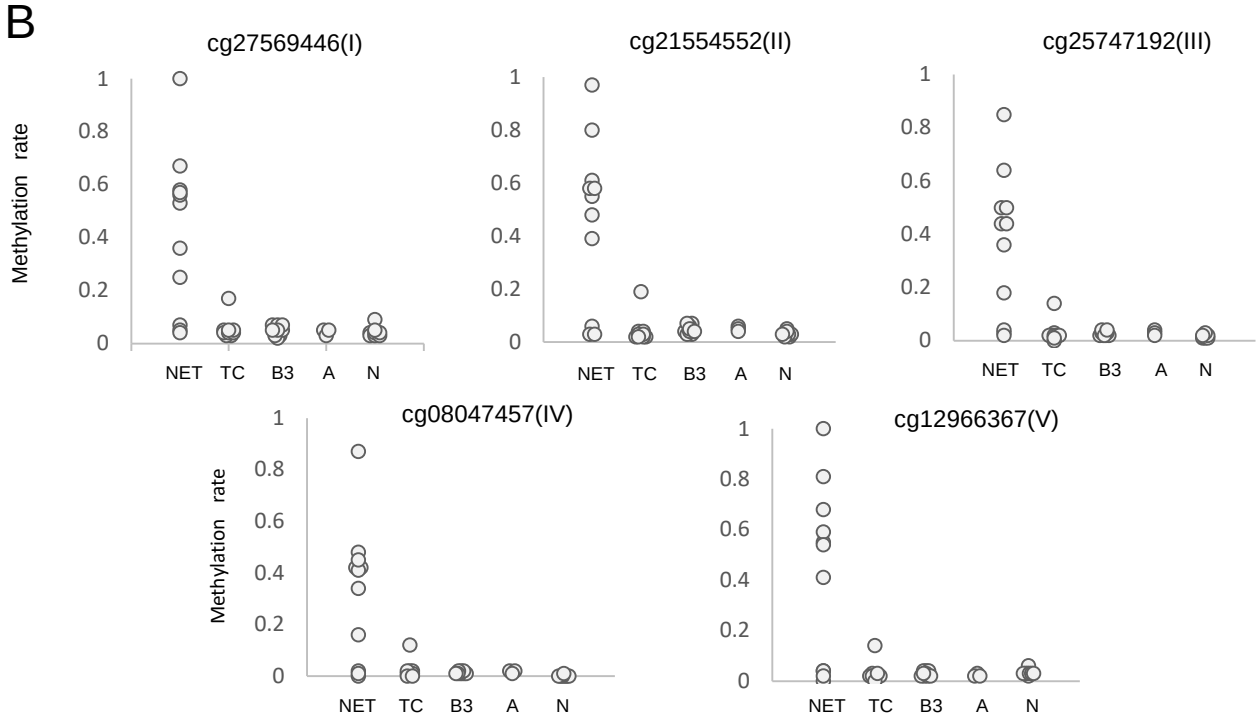
B
cg27569446(I)
cg21554552(II)
cg25747192(III)
cg08047457(IV)
cg12966367(V)
Methylation rate
1
0.8
0.6
0.4
0.2
0
NET
TC
B3
A
N

Figure 3

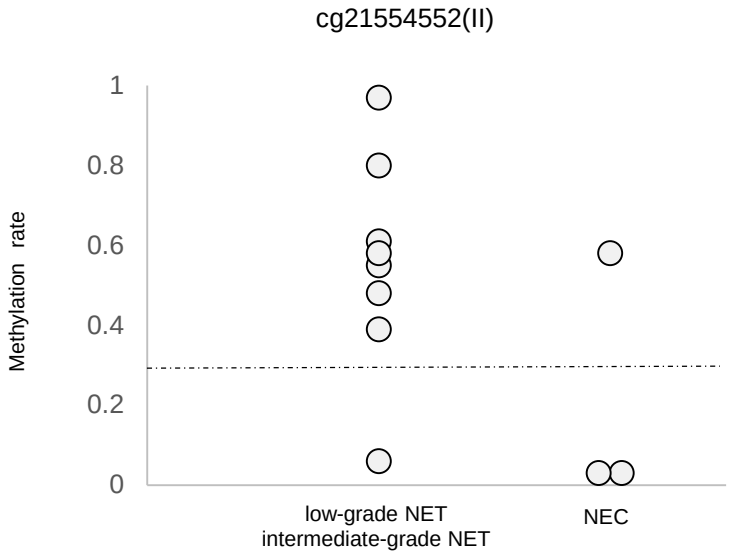

	low-grade intermediate-grade NET	NEC
methylation	7	3
unmethylation	1	2

$p=1.53 \times 10^{-9}$

Figure 4

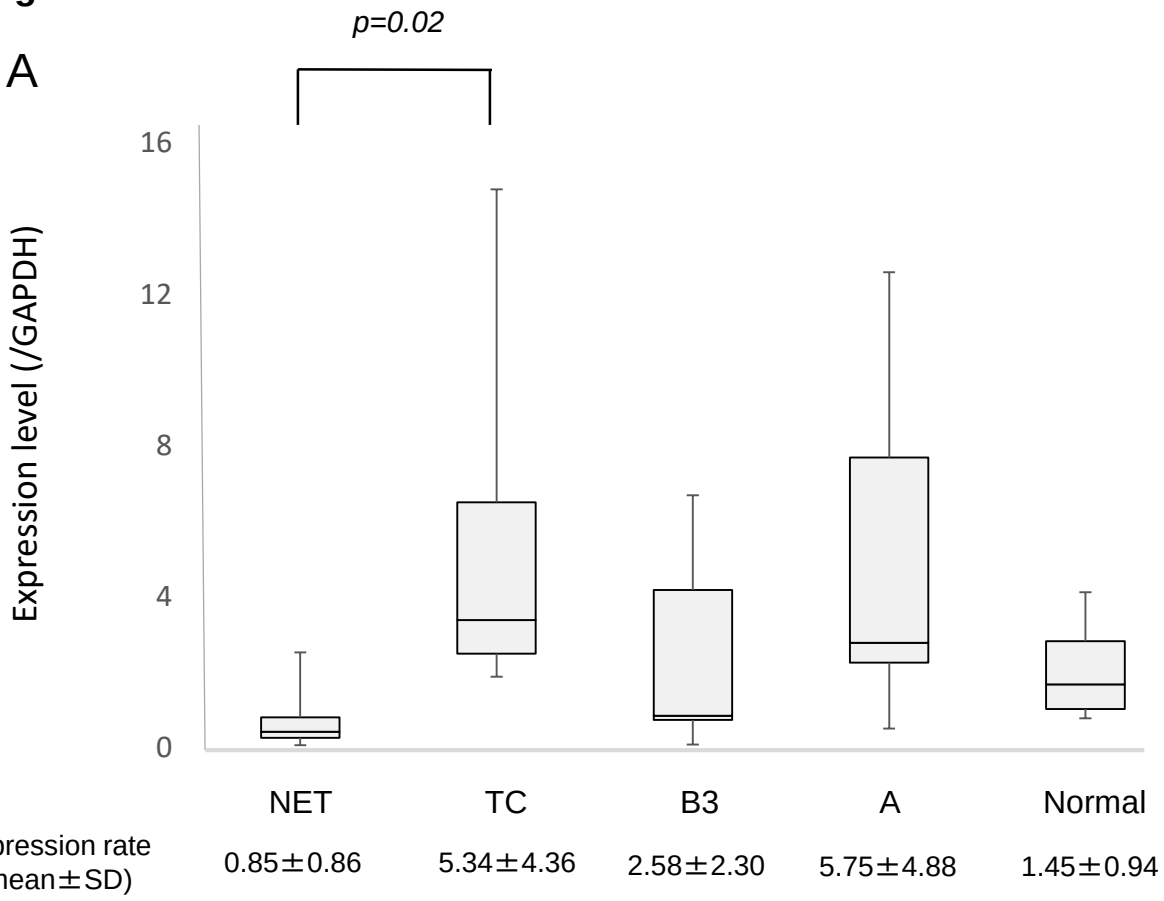
A
p=0.02
Expression level (/GAPDH)
16
12
8
4
0
NET
TC
B3
A
Normal
Expression rate (mean±SD)
0.85±0.86
5.34±4.36
2.58±2.30
5.75±4.88
1.45±0.94

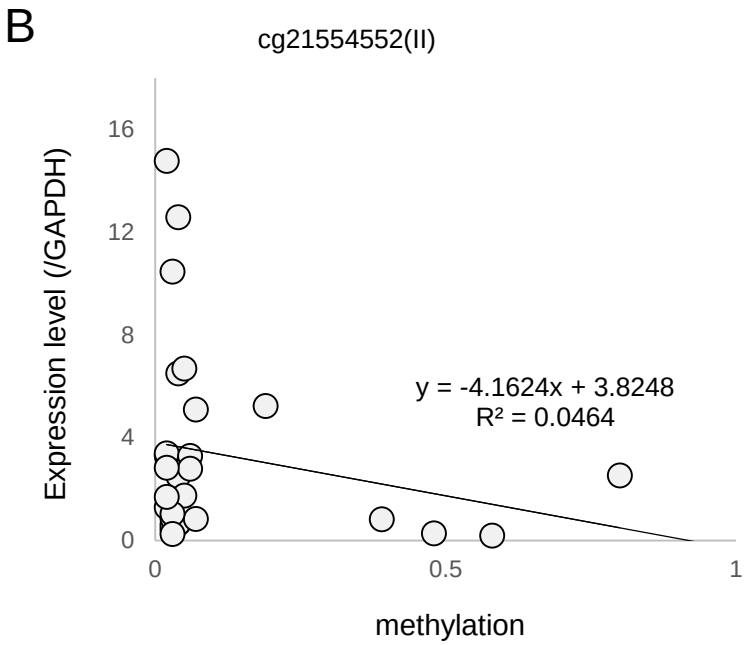
B
cg21554552(II)
Expression level (/GAPDH)
16
12
8
4
0
y = -4.1624x + 3.8248
R² = 0.0464
0
0.5
1
methylation

Figure 5

A

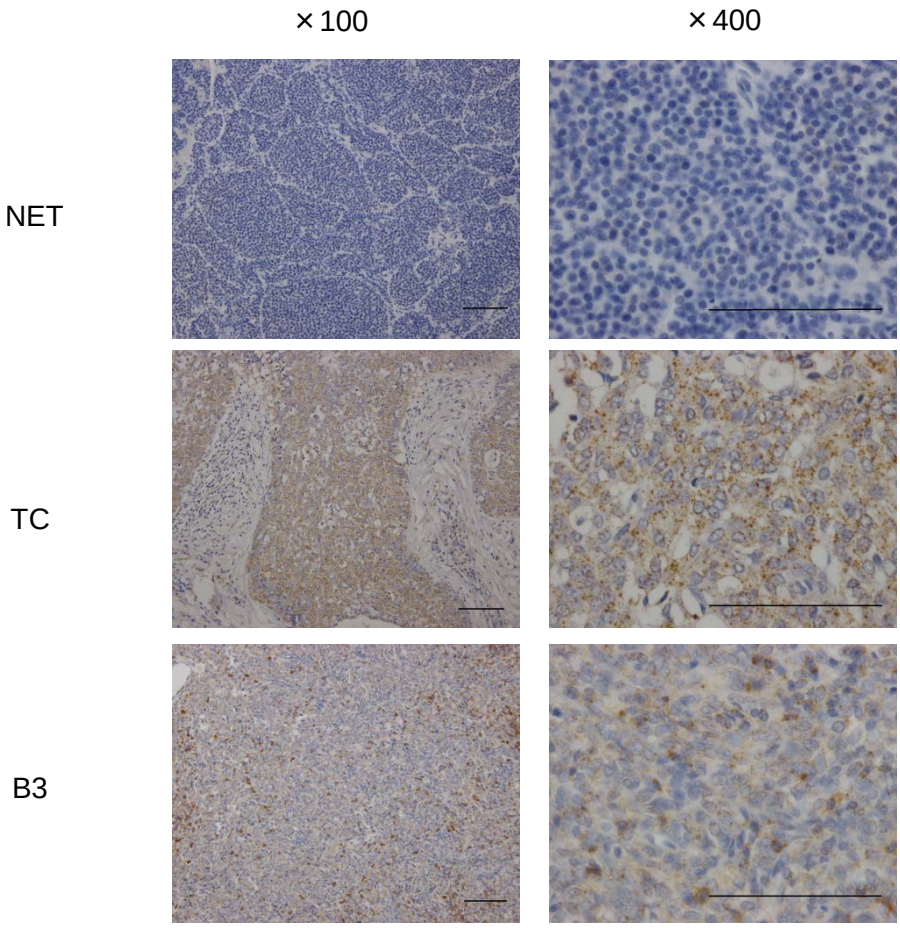

B

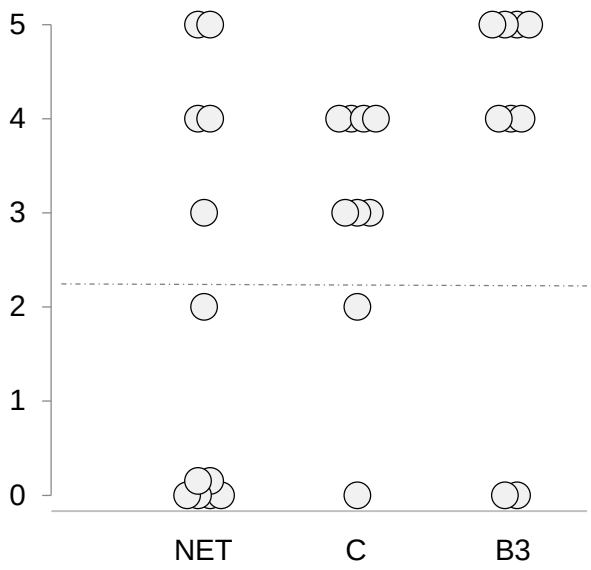

scoring
Stain intensity
strong : 2
weak : 1
none : 0
Stain expanding
diffuse(>80%) : 3
moderate (50-80%) : 2
focal (20-50%) : 1
none (<20%) : 0

Score ≦2 inhibition
Score ≧3 normal

RASSF1	expression	inhibition rate
NET	7/12	(58.3%)
C	2/9	(22.2%)
B3	2/9	(22.2%)

p=0.003

Table 1. Clinicopathological characteristics of patients with thymic epithelial tumor used screening genome-wide methylation assay

group	histology	age	gender (M:F)	with MG	Masaoka classification	
NET	(n=3)					
	low-intermediate-grade NET	58.7±5.6 (51-64)	2:1	0	1	n=1
					3	n=1
					4b	n=1
TC	(n=7)					
	squamous cell carcinoma	59.1±5.2 (51-69)	3:4	0	2	n=3
					3	n=1
					4a	n=1
					4b	n=1
B3	(n=8)					
	type B3 thymoma	57.9±17.2 (28-75)	2:6	2	1	n=2
					2	n=1
					3	n=3
					4a	n=2

Table S1. Clinicopathological characteristics of patients with thymic epithelial tumor used methylation and expression analysis in this study

			patient					Sample for analysis			
sample ID	group ID	biospecimen	age	gender	MG	Masaoka classification	histology / WHO classification	methylation screening (Human methylation 450K)	methylation (pyrosequence)	expression (RT-PCR)	expression (immunohistochemistry)
1	NET	frozen	51	F	-	3	carcinoid / low-inetmediate-grade NET	○	○	○	○
2	TC	frozen	55	M	-	2	squamous cell carcinoma	○	○	○	○
3	TC	frozen	51	F	-	2	squamous cell carcinoma	○			○
4	A	frozen	50	F	-	1	thymoma type A	○	○	○	
5	TC	frozen	60	M	-	2	squamous cell carcinoma	○	○	○	○
6	TC	frozen	58	F	-	4	squamous cell carcinoma	○	○	○	○
7	TC	frozen	69	F	-	4b	squamous cell carcinoma	○	○	○	○
8	TC	frozen	60	F	-	4a	squamous cell carcinoma	○			○
9	B3	frozen	66	M	-	1	thymoma type B3	○	○	○	○
10	B3	frozen	28	F	+	4a	thymoma type B3	○	○	○	○
11	B3	frozen	75	F	-	1	thymoma type B3	○	○	○	○
12	B3	frozen	64	M	-	2	thymoma type B3	○	○		○
13	NET	frozen	61	M	-	1	carcinoid / low-inetmediate-grade NET	○	○	○	○
14	B3	frozen	36	M	+	4a	thymoma type B3	○	○	○	
15	B2	frozen	50	F	+	3	thymoma type B2		○		
16	TC	frozen	61	M	-	3	squamous cell carcinoma	○	○	○	○
17	NET	frozen	64	M	-	4b	atypical carcinoid / inetmediate-grade NET	○	○	○	○
18	B3	frozen	47	M	-	3	thymoma type B3	○	○	○	○
19	A	frozen	62	M	-	1	thymoma type A	○	○	○	
20	B3	frozen	75	M	-	3	thymoma type B3	○	○	○	○
22	NET	frozen	67	F	-	4b	small cell carcinoma / high-grade NEC		○	○	○
23	B3	frozen	72	M	-	3	thymoma type B3	○	○	○	○
24	A	frozen	80	F	-	1	thymoma type A	○	○	○	
25	TC	frozen	61	F	-	2	squamous cell carcinoma		○	○	○
27	B2	frozen	74	F	-	2	thymoma type B2		○	○	
28	B2	frozen	65	F	-	2	thymoma type B2		○	○	
31	B2	frozen	75	F	-	2	thymoma type B2		○		
33	TC	frozen	68	F	-	2	squamous cell carcinoma		○	○	○
34	B3	frozen	68	F	+	2	thymoma type B3		○	○	○
35	TC	frozen	69	M	-	2	squamous cell carcinoma		○	○	
36	B1	frozen	65	F	-	1	thymoma type B1		○		
37	TC	frozen	48	F	-	3	squamous cell carcinoma		○	○	
38	B2	frozen	40	F	-	2	thymoma type B2		○	○	
39	B2	frozen	52	F	+	2	thymoma type B2		○	○	
40	B2	frozen	60	F	-	1	thymoma type B2		○	○	
41	B1	frozen	84	M	-	2	thymoma type B1		○		
42	B1	frozen	51	F	+	2	thymoma type B1			○	
43	B1	frozen	71	F	-	2	thymoma type B1			○	
44	B1	frozen	72	F	-	1	thymoma type B1		○	○	
45	AB	frozen	67	F	+	1	thymoma type AB			○	
46	AB	frozen	58	M	-	2	thymoma type AB			○	
47	AB	frozen	65	F	-	2	thymoma type AB		○	○	
48	AB	frozen	56	F	+	2	thymoma type AB			○	
49	AB	frozen	74	F	-	1	thymoma type AB			○	
50	NET	frozen	68	M	-	2	typical cartinoid / low-grade NET		○	○	○
51	NET	FFPE	53	M	-	unknown	cartinoid		○		○
52	NET	FFPE	61	M	-	unknown	cartinoid		○		○
53	NET	FFPE	71	M	-	unknown	cartinoid		○		○
54	NET	FFPE	45	F	-	unknown	atypical carcinoid / inetmediate-grade NET		○		○
55	NET	FFPE	70	F	-	unknown	high-grade NEC		○		○
56	NET	FFPE	49	M	-	unknown	high-grade NEC		○		○
57	Non-tumor	frozen	58	F	-	-	normal thymus (case6)		○		
58	Non-tumor	frozen	80	F	-	-	normal thymus (case24)	○			
59	Non-tumor	frozen	61	F	-	-	normal thymus (case25)		○	○	
60	Non-tumor	frozen	74	F	-	-	normal thymus (case27)		○	○	
61	Non-tumor	frozen	65	F	-	-	normal thymus (case28)		○	○	
62	Non-tumor	frozen	40	M	+	-	normal thymus (case30)		○	○	
63	Non-tumor	frozen	69	M	-	-	normal thymus (case35)		○		
64	Non-tumor	frozen	48	F	-	-	normal thymus (case37)		○		
66	Non-tumor	frozen	68	M	-	-	normal thymus (case50)			○	
65	Non-tumor	FFPE	49	M	-	-	normal thymus (case55)		○		

Table S2. Top of 15 CpG islands significantly hypermethylated in NET compared to squamous cell carcinomas

		Methyaltion status of CpG island		CpG island-related RefSeq gene	
Rank	CpG island	Adjusted p-value	beta.Difference	Gene name	Location of CpG island
1	chr1:2222198-2222569	4.81E-10	0.6983	SKI	Gene body
2	chr19:11533198-11533619	9.62E-10	0.6095	CCDC151	Gene body
3	chr17:41363727-41364273	7.59E-08	0.7567	TMEM106A	Exon 1
4	chr12:57635240-57635572	1.51E-05	0.5032	NDUFA4L2	upstream
5	chr4:169753048-169754535	1.51E-05	0.5823	PALLD	Gene body
6	chr7:75896510-75896944	1.51E-05	0.7600	SRRM3	Gene body
7	chr19:41115445-41115767	1.04E-04	0.5224	LTBP4	Gene body
8	chr19:38885233-38885505	1.56E-04	0.6203	SPRED3	Gene body
9	chr3:50377803-50378540	1.60E-04	0.5323	RASSF1	Exon 1
10	chr12:132690339-132690571	2.84E-04	0.6605	GALNT9	Exon 1
11	chr2:242549373-242549995	2.84E-04	0.5121	THAP4	Gene body
12	chr19:47139337-47139547	2.95E-04	0.5784	GNG8	upstream
13	chr2:120190030-120190308	2.95E-04	0.5812	TMEM37	Gene body
14	chr16:374732-375328	3.09E-04	0.6649	AXIN1	Gene body
15	chr11:119613005-119613521	3.40E-04	0.5138	RGL3	upstream

Table S3. Top of 15 CpG islands significantly hypermethylated in NETs compared to type B3 thymomas

		Methyaltion status of CpG island		CpG island-related RefSeq gene	
Rank	CpG island	Adjusted p-value	beta.Difference	Gene name	Location of CpG island
1	chr1:2222198-2222569	3.84E-12	0.6974	SKI	Gene body
2	chr17:41363727-41364273	1.78E-09	0.7593	TMEM106A	Exon 1
3	chr19:42386865-42387485	7.38E-08	0.5052	ARHGEF1	Gene body
4	chr19:47507306-47507692	2.36E-07	0.5583	GRLF1	upstream
5	chr2:120190030-120190308	5.68E-07	0.6231	TMEM37	Gene body
6	chr7:75896510-75896944	8.45E-07	0.7492	SRRM3	Gene body
7	chr18:35104533-35104942	2.39E-06	0.5470	BRUNOL4	Gene body
8	chr19:41115445-41115767	2.52E-06	0.5350	LTBP4	Gene body
9	chr7:75889086-75889345	2.75E-06	0.7061	SRRM3	Gene body
10	chr4:169753048-169754535	3.83E-06	0.5706	PALLD	Exon 1
11	chr2:242549373-242549995	9.01E-06	0.5419	THAP4	Gene body
12	chr9:139580969-139582615	9.55E-06	0.5153	AGPAT2	Exon 1
13	chr19:11533198-11533619	1.23E-05	0.5828	CCDC151	Body
14	chr3:50377803-50378540	1.24E-05	0.6013	RASSF1	Exon 1
15	chr19:47139337-47139547	1.34E-05	0.5205	GNG8	upstream

Table S4. List of primer sets used in TaqMan and antibody in immunochemistry.

Gene/primer name		Sequence/ID
Pyrosequencing for RASSF1		
	Forward	5'-ATTTGGGTGTAGGGATTGTG-3'
	Reverse	Biotin-5'-AACTAACCTCCAAAAACACAAAT-3'
	Sequence	TGTAGGGATTGTGGG
TaqMan gene expression assay*		
RASSF1	FAM	Hs00296057_m1
GAPDH	FAM	Hs02758991_g1

ID	dilution	Vender
Immunohistochemistry for RASSF1		
ab23950	1:500	Abcam plc, Cambridge, UK

* TaqMan gene expression assay were produced by Thermo Fisher SCIENTIFIC(Yokohama, Japan)